AGU PUBLICATIONS

Geophysical Research Letters

RESEARCH LETTER
10.1002/2017GL074882

Key Points:
- We estimate that ARs contribute to about 22% of total global runoff with a number of regions reaching 50% or more
- In several regions ARs are linked with up to 80% of floods; ARs absence may increase up to 90% the frequency of hydrological droughts events
- Globally, we find that ~300 million people are exposed to additional flood and drought risk due to ARs

Supporting Information:
- Supporting Information S1

Correspondence to:
H. Paltan,
homero.paltanlopez@ouce.ox.ac.uk

Citation:
Paltan, H., Waliser, D., Lim, W. H., Guan, B., Yamazaki, D., Pant, R., & Dadson, S. (2017). Global floods and water availability driven by atmospheric rivers. *Geophysical Research Letters*, *44*, 10,387–10,395. https://doi.org/10.1002/2017GL074882

Received 20 JUL 2017
Accepted 4 OCT 2017
Accepted article online 9 OCT 2017
Published online 25 OCT 2017

Global Floods and Water Availability Driven by Atmospheric Rivers

Homero Paltan[1,2], Duane Waliser[2], Wee Ho Lim[3,4], Bin Guan[2,5], Dai Yamazaki[6,7], Raghav Pant[3], and Simon Dadson[3]

[1]School of Geography and the Environment, University of Oxford, Oxford, UK, [2]NASA Jet Propulsion Laboratory, California Institute of Technology, Pasadena, CA, USA, [3]Environmental Change Institute, University of Oxford, Oxford, UK, [4]Institute of Geographic Sciences and Natural Resources Research, Chinese Academy of Sciences, Beijing, China, [5]Joint Institute for Regional Earth System Science and Engineering, University of California, Los Angeles, CA, USA, [6]Institute of Industrial Science, University of Tokyo, Tokyo, Japan, [7]Department of Integrated Climate Projection Research, Japan Agency for Marine-Earth Science and Technology, Yokohama, Japan

Abstract While emerging regional evidence shows that atmospheric rivers (ARs) can exert strong impacts on local water availability and flooding, their role in shaping global hydrological extremes has not yet been investigated. Here we quantify the relative contribution of ARs variability to both flood hazard and water availability. We find that globally, precipitation from ARs contributes 22% of total global runoff, with a number of regions reaching 50% or more. In areas where their influence is strongest, ARs may increase the occurrence of floods by 80%, while absence of ARs may increase the occurrence of hydrological droughts events by up to 90%. We also find that ~300 million people are exposed to additional floods and droughts due the occurrence of ARs. ARs provide a source of hydroclimatic variability whose beneficial or damaging effects depend on the capacity of water resources managers to predict and adapt to them.

1. Introduction

Key water resources and flood risk management decisions depend on our understanding of drivers of hydrological variability (Blöschl et al., 2007; De Loe & Kreutzwiser, 2000; Gleick, 1989; Trenberth, 2005). The magnitude and timing of runoff responds to hydroclimatic variability across subseasonal to interannual timescales. This variability is strongly connected to the large-scale transport of moisture in the atmosphere which is in part controlled by large-scale atmospheric modes of variability such as El Niño–Southern Oscillation, North Atlantic Oscillation, Pacific/North American teleconnection, and the Indian Ocean Dipole (Kenyon & Hegerl, 2010; McCabe & Palecki, 2006; Mestas-Nuñez & Enfield, 1999; Viles & Goudie, 2003). Apart from these large-scale modes, regional and local-scale climates also modulate narrow, elongated corridors of enhanced water vapor transport in the lower troposphere, known as atmospheric rivers (ARs) (Guan et al., 2013; Guan & Waliser, 2015). ARs are understood to be responsible for over 90% of the total tropical-temperate vertically integrated horizontal water vapor flux (Dacre et al., 2015; Ghanbarian-Alavijeh et al., 2010; Gimeno et al., 2014; Guan & Waliser, 2015; Zhu & Newell, 1998). Their typical horizontal dimensions might be several thousand kilometers long with width ~500 km (Ralph & Dettinger, 2011), and at any given time there may be 3–5 ARs in each hemisphere (Zhu & Newell, 1998).

Several prior analyses have documented the local implications for water resources of AR-driven precipitation. For instance, in the West Coast of the U.S. and in Europe, ARs supply on average about 30% of total precipitation (Lavers & Villarini, 2015) leading to peak historical floods in Washington state (Lavers & Villarini, 2015; Neiman et al., 2011; Ralph & Dettinger, 2011). Also, the influence of these rains on water supplies has been quantified in California where ARs contribute 30–50% of river flow (Dettinger, 2011). In Europe, AR-triggered rainfall has been observed in the Iberian Peninsula, Norway, Poland, France, and Great Britain, where ARs have been found to contribute to extreme winter flooding (Lavers & Villarini, 2015; Ramos et al., 2016). In the Southern Andes they are also thought to drive ~80% of total winter precipitation (Viale & Nuñez, 2011). Globally, a recent study has documented considerable hitherto unknown landfall and inland penetration of ARs in areas with less extensive records, such as Southeast Asia, South America, South Africa, Australia, and Central Europe (Guan & Waliser, 2015). Thus, the new global areas of AR landfall and penetration, along with the previous documented strong local influence of ARs suggest that ARs may be an important driver of global terrestrial hydrology.

In this paper, we utilize a global AR database to evaluate for the first time the following question: what is the influence of these horizontal moisture transport extremes in shaping global land surface hydrology and its variations? To answer this question, we first quantify the contribution of ARs to global runoff, to soil moisture content, and to snowpack size. Next, using a uniform observation and modeling methodology, we identify new regions and catchments of the globe where ARs dominate the magnitude and occurrence of hydrological droughts and floods. Lastly, we calculate the additional population exposed to hydrological drought and flood hazards due to ARs.

2. Methods and Data

2.1. Land Surface Hydrology

We run a Land Surface Model (LSM) in order to generate snow water equivalent, total runoff, and total soil moisture under *control* meteorological conditions. For this we force the Joint UK Land Exchange Scheme (JULES) (for details see Best et al., 2011, and Blyth et al., 2006) with the meteorology obtained from the latest WFDEI global gridded reanalysis product covering the period 1979–2010 (GPCC corrected) (Weedon et al., 2014) and the default configuration of the model. Soil properties are obtained from the Harmonized World Soil Database from FAO-IIASA (Fischer et al., 2012), and the hydraulic soil properties used here are derived following the method of Cosby et al. (1984). The temporal time step of our control meteorological conditions is 3 h, and the spatial resolution is 0.5° × 0.5°. In our *perturbed* simulation we derive AR precipitation values based on a global AR database (Guan & Waliser, 2015) and then we subtract the precipitation fraction corresponding to ARs for this at each time step. The difference between the control and perturbed runs is in the precipitation forcing. At any given time step, the control run is driven by a global map of the reanalysis precipitation. The perturbed run is driven by a version of the reanalysis precipitation where precipitation falling inside of detected AR boundaries during that time step is removed. Also, various AR detection techniques exist in the literature, often emphasizing different aspects of ARs and indicative of complementing views on the AR definition. In this study, we take a broad definition of ARs, which, as in Zhu and Newell (1998), does not limit the existence of ARs to the extratropics or by any other regional requirements.

In both cases, we use the default configuration of JULES which, when given total precipitation, partitions rainfall and snowfall at the given near-surface air temperature of 274.0 K. Precipitation below this threshold is assumed to be snowfall. We also activate the default multilayer scheme model in JULES, which permits a maximum of three layers (snow depths of 0.1, 0.15, and 0.2 m) where the density of fresh snow is set to 100 kg m^{-3}. This model also partitions snowfall between that which is intercepted by the canopy and that which falls beneath it and uses a spectral scheme to calculate snow albedo. The default configuration represents soils with four vertical layers, each with its own temperature and soil moisture. Runoff is generated using TOPMODEL, which has been shown to provide a detailed physical representation of the basin leading to improved simulations of the seasonal peaks, subsurface runoff, and dry season flows (Clark & Gedney, 2008). The topographic supporting data sets for TOPMODEL is calculated using an improved topographic index based on a 15 arc sec resolution global map (Marthews et al., 2015).

2.2. River Routing and Hydrological Extremes

Daily generated runoff from both the control and perturbed simulations are used to drive the CaMa-Flood model (Yamazaki et al., 2011) in order to generate daily river discharge at a spatial resolution of 0.25° × 0.25°. At each grid location, the annual maxima of river discharge are extracted from the computed daily values. Then these annual maxima are fitted using a two-parameter Gumbel distribution following previous studies (Dankers & Feyen, 2009; Gumbel, 1941; Hirabayashi et al., 2013).

For consistency with conventional practice in hydrology, we define the threshold for droughts and floods in terms of flow duration percentiles, which are quoted as exceedance probabilities. We define the threshold for hydrological drought as the flow which is exceeded 90% of the time (hereinafter referred to as Q90) (Sheffield & Wood, 2011; Van Loon, 2015). We define the high flow threshold as that flow which is exceeded 10% of the time (referred to as Q10). Then a change in extreme discharge magnitude was calculated as percentage in change in the hydrological thresholds, Q90 and Q10, between the control and perturbed simulation. Thus, the contribution of ARs to low and high flows are obtained as the change in the magnitude of the return

period of river discharge for Q90 and Q10 flows, respectively. In our analyses, we do not account for human interventions and flow regulations such as dams or reservoirs.

Next, we assessed how the presence of ARs increase the periodicity of exceedance of hydrological droughts and floods events. So we follow a similar approach used by Dettinger and Cayan to assess the role of ARs in fluctuations of drought episodes in the California Delta (Dettinger & Cayan, 2014). We first aggregate the gridded daily river discharge into monthly subsets for both the control and the disturbed simulation. Later, a rule is applied that if the minimum value within an aggregate is less than the Q90 value (obtained from previous steps), the aggregate is considered as one with an event of hydrological drought. Similarly, if the maximum value within an aggregate is seen to exceed the Q10 value, we consider such aggregate as one with a high flow. So for each grid location, and simulation, we obtain a record of the frequency of events that were categorized as hydrological drought or flood. For each grid location, we then calculate how the absence of ARs increases the occurrence of hydrological drought events and how the presence of ARs increases the occurrence of high flows events.

2.3. Exposure to Droughts and Floods

We calculate the number of people exposed to areas with strong hydrological drought and flood signals driven by variability of ARs storms. For droughts, we define the signal as strong in locations where the absence of ARs increase the occurrence of droughts events by more than 50%. We then delineate catchment boundaries using data from GRDC (Global Runoff Data Centre, 2007). From here, we select those catchments where the drought signal is dominant. We estimated the population exposed to droughts by overlaying a gridded population data set provided by GPWv4 (Center for International Earth Science Information Network—CIESIN—Columbia University, 2016) with the pattern of catchments showing a strong AR-driven drought signal.

Last, in order to calculate people exposed to floods driven by ARs, we compute flood hazard maps from both, the *control* and the *perturbed* simulations. Flood hazard is computed using the close relationship, given by a cumulative distributive function, between flooded area and floodplain water depth or total water storage (sum of river and floodplain storage) (Yamazaki et al., 2011). For this, we fit the two-parameter Gumbel distribution using the annual maxima of river water depth maxima (which is used as proxy for total water storage). From this distribution, we derive the 100 year flood inundation fractions for both simulations. We then estimate the increase in flooded area due to ARs. Using the GRDC data, we then calculate the population exposed to AR-driven floods by multiplying the population of each grid by the fraction of its flooded area.

3. Results

3.1. Land Surface Hydrology

The mean annual contribution of ARs to global runoff is 22% (Figure 1a). ARs contribute more than 50% of the mean annual runoff on the east and west coasts of North America, the southeastern part of South America, location in the south of Chile, France, northern Spain and Portugal, the United Kingdom, Southeast Asia, and New Zealand. The inland advection of moisture associated with ARs exerts a smaller influence (less than 30% of mean annual runoff) on the spatial pattern of runoff in southern parts of the Amazon basin, southern Africa, and India. Moreover, ARs contribute an additional 15–25% to soil moisture in these areas as well as in Australia, Iran, and continental Europe (Figure 1b).

The moisture associated with ARs also exerts a significant control on the accumulation of the snowpack in the Northern Hemisphere (but notably not in western Europe; Figure 1c). Our analysis is in agreement with earlier local results that ARs contribute approximately 40% of the moisture stored in the snowpack of the Sierra Nevada mountain range (Guan et al., 2013), but we demonstrate here that their influence is much wider. We also show a yearly contribution to the snowpack that ranges between 25 and 50% in areas extending to Alaska, Quebec, the Pontic Mountains in Turkey, and the Altai and Hangai Mountains in Mongolia (Figure 1c). In mountainous areas, our findings indicate that precipitation driven by ARs supplies approximately 34% of the snowpack throughout the year in the Alps, 11% in the Himalayas, and 68% in the Southern Andes (see supporting information Figure S1).

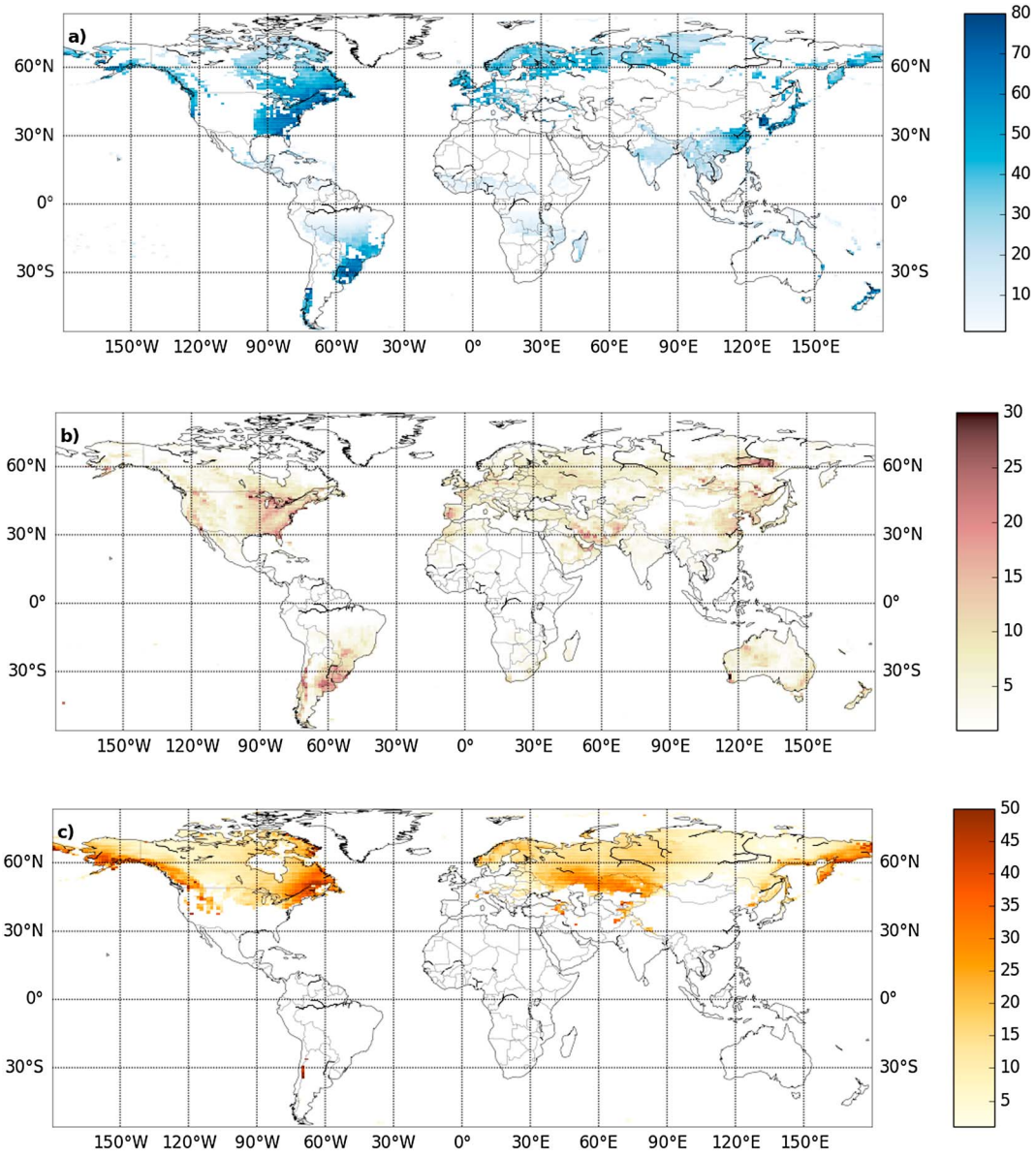

Figure 1. Mean annual contribution of ARs to hydrological land surface variables. Mean annual (1979–2010) contribution (%) of ARs to (a) runoff, (b) total soil moisture content, and (c) snow water equivalent.

3.2. Contribution of ARs to the Intensity of Extreme Flows

The contribution of ARs to flow extremes across global major catchments is shown in Figure 2. The catchments where the impact is most notorious are located in extratropical regions (north of 30°N and south of 30°S) including rivers in the California's Central Valley, inland catchments in the south of South America, the Iberian Peninsula (Douro catchment), in Turkey and Iran (for example, Great Kivar in Iran and Dicle Firat in Turkey), and the Murray-Darling in Australia. In these catchments, the contribution ARs typically contribute to >80% to both low and high flows. Also, in catchments such as the Thames (UK) and the Escaut (France-Belgium) the contribution of ARs to low flow is ~80% despite showing smaller contributions to the high flow (about 40%). Also, catchments where ARs contribute considerably (~50%) to both high and low flows are found along the coast of the Gulf of Mexico in the U.S., the Uruguay river in South America, the Colorado in Argentina, the Seine and Rheine in Europe, the Tigris-Euphrates and Aral in Eurasia, and the Amur in Asia (Russia and China). Also, significant contributions to extreme flows (~40%) can be found in several major

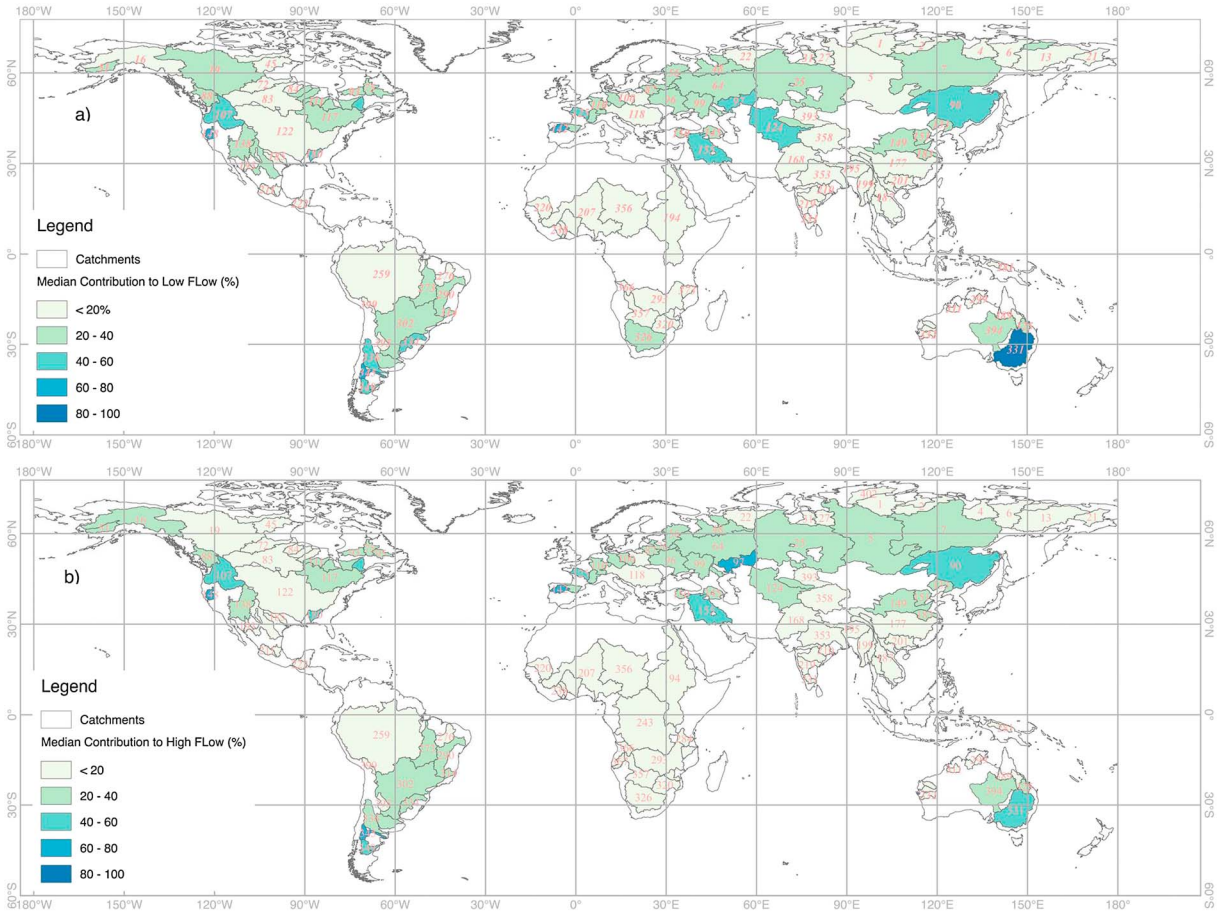

Figure 2. Median contribution of ARs to extreme flows: (a) low flows and (b) high flows. Low flow is defined here as the Q90 flow, so this is the flow that is expected to be equaled or exceed 90% of the time. High flow is defined here as the Q10 flow, so this is the flow that is expected to be equaled or exceeded 10% of the time. Period 1979–2010. Contributions of <1% were removed, and also, catchments with a drainage area < 75 km^2 are not shown here. A list of catchments IDs and values for the catchments not shown in this figure is presented supporting information Table S1.

catchments such as the Parana in Brazil, the Po and Elbe in Europe, catchments in Siberia, and several catchments in China. A smaller regional influence (<20%) is found in tropical basins such as the Mississippi in the U.S., the Amazon, catchments in Central America, the Congo and other African rivers, and the south of Asia including the Himalayan-fed catchments. Nonetheless, other several small catchments show also an important impact of ARs (supporting information Figure S2). For example, we detect that in several areas in the UK, New Zealand, and Australia, ARs may contribute to up to 80% of high and low flows. Similarly, in large catchments such as the Mississippi, the Paraná in Brazil, and Amur, we detect high standard deviations (~30) in our catchment measures (see supporting information Table S1) which reflects very important contributions (80%) to high flows in several sections of such catchments. Our findings are also demonstrated by calculating flow duration curves of six catchments, across different regions, where we have detected a major influence of ARs; see supporting information Figure S3. For instance, in the Sacramento catchment, flows of 1,000 m3/s are likely to be exceeded less than 5% of the time when there are no ARs. By contrast, in the presence of AR-driven precipitation, the likelihood of river flow exceeding 1,000 m^3/s increases to approximately 20%. In contrast, the likelihood of exceedance of the reference low flow of this river (210 m^3/s) decreases from 90% when ARs are present, to 60% when they do not make landfall.

3.3. Contribution of ARs to the Occurrence of Droughts and Floods

The role of ARs in the occurrence of events of hydrological droughts and floods is shown in Figure 3. We detect that in several temperate catchments the frequency of periods of hydrological drought increases when AR-driven moisture fluxes are absent (Figure 3a). In the most significant cases, the absence of ARs

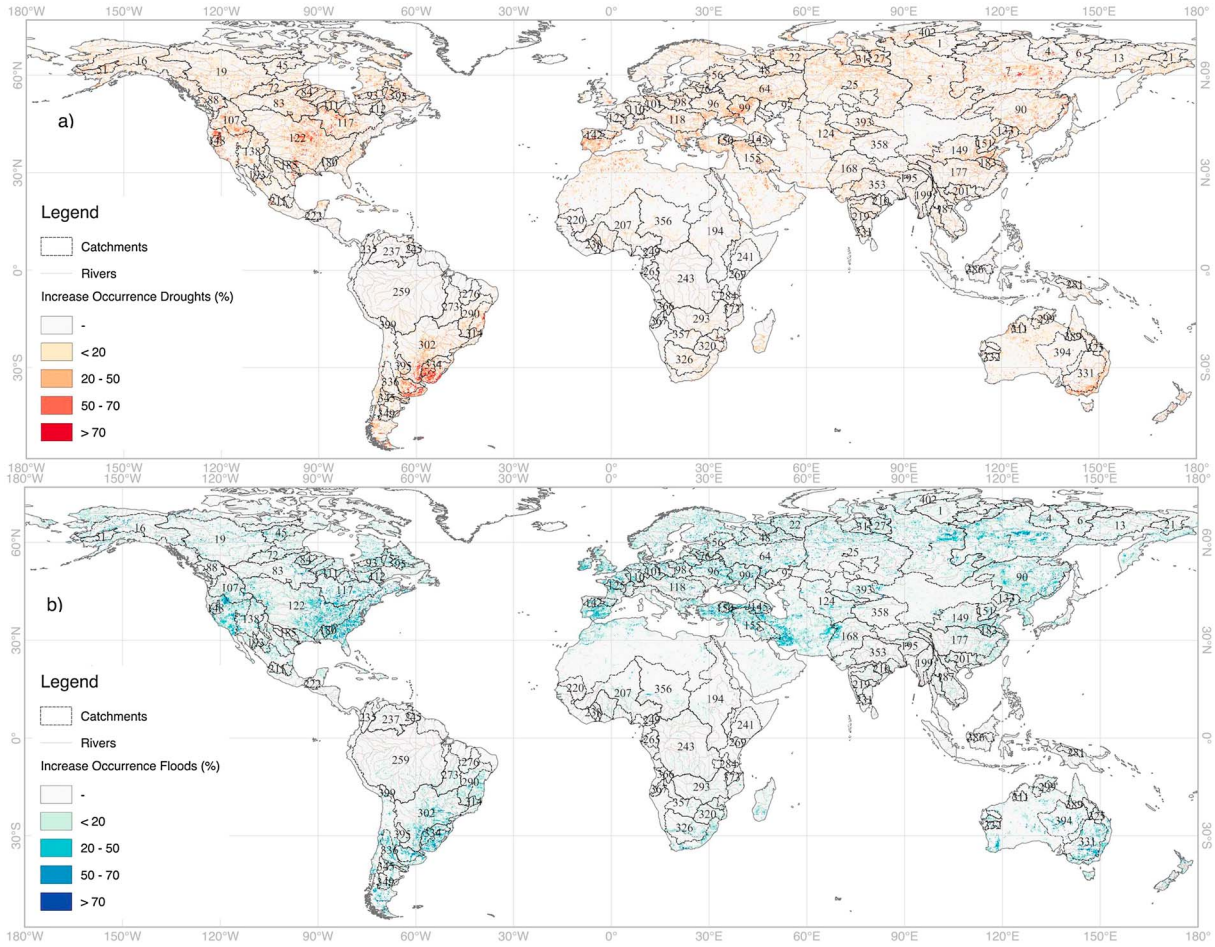

Figure 3. Role of ARs in the frequency of occurrence of hydrological droughts and floods: (a) increase in the occurrence of droughts events due to the absence of ARs and (b) increase in the occurrence of flood events due the presence of ARs. A hydrological drought event is detected when, within a monthly aggregate of daily flows, its minimum value is observed to be below the Q90 threshold. A flood event is detected when, within a monthly aggregate of daily flows, its maximum value is observed to be above the Q10 threshold. Total increase in the occurrence of events for the period 1979–2010. Catchments with drainage area < 75 km^2 are not labeled. A list of catchment ID is presented in supporting information Table S1.

can increase the frequency with which such hydrological drought events occur by up to 90%. Regions where this behavior is observed include the Central Valley in California (previously documented by (Dettinger & Cayan, 2014)), the Missouri River in the U.S., the Canadian shield, the Parana, the Iberian Peninsula, the Mediterranean coast of Europe, the Amur in Russia and China, the area around the Black Sea, north of in Iran, and the Yellow River in Asia. A strong signal is also detected in the Murray-Darling outlets and in New Zealand. Also, in the Orange River of South Africa and in the Indus basin an important impact of the absence of ARs is also identified. Lastly, we observe a minor influence of ARs in low flow episodes in Arctic basins such as the Ob and the Yukon area, in Russia (20%).

The role of AR-driven fluxes in increasing the periodicity of high flow events is shown in Figure 3b. This observed signal is more widespread than that for hydrological droughts. For instance, in the Central Valley in California (particularly in the upper parts and at the coastal ends of those catchments), periods of high flows follow closely the variation in the occurrence of ARs. Such strong signal has been previously detected by, for example, Ralph et al. (2006) who attributed flood events between 1997 and 2004 in the Russian River, California to AR conditions. Similarly, Neiman et al., 2011 found a close link between AR landfall and annual peak daily flows in Western Washington between 1980 and 2009. We also find that on the North American east coast, ARs increase the occurrence of flooding events in the Mississippi river and in other several small catchments. In addition, ARs significantly impact the occurrence of high flows in Turkey, Spain, and France (in the Seine and Loire Rivers ARs have increased the occurrence of high flow events by 80%). Also in Britain,

Germany (e.g., the Rhine River), and in Eastern Europe, ARs may increase the occurrence of high flows by 40%. A similar pattern is observed in Central Asia and in China (up to 50% in the lower parts). In Australia and New Zealand, the signal is confined to coastal regions, for example, in the Murray-Darling basin ARs increased by 80% the occurrence of high flow events. In Africa, we find a significant signal in north and southeast Africa, for example, in Morocco (the Moulouya River, 40%) and in the Orange River in South Africa (up to 25%).

3.4. Societal Risks and Hazard Associated With Atmospheric Rivers

We calculate the population exposed to droughts and flood hazards that stem from ARs by representing detected high and low flow episodes across major global catchments (see supporting information Figure S4). We detect that on average approximately 350 million people have been directly exposed to hydrological droughts that may result from the occurrence of ARs. The catchments with the greatest exposed populations are the Parana and Uruguay Rivers, the Mississippi (principally around the Missouri tributary) and the St. Lawrence Rivers in the U.S., and the Dnieper and Don basins in Eurasia (especially in the region between Russia and Ukraine).

By contrast, approximately 300 million people across the globe are exposed to additional flood risk due to the occurrence of ARs. The most significant areas with increased exposure are found in California, the Mississippi basin, in the Parana River, in Iberian Peninsula, southern Iran, the Amur and Yangtze Rivers, and the Murray-Darling basins (see supporting information Figure S5). This finding suggests that improved understanding, and in turn modeling and prediction capabilities, of the way in which ARs influence hydrometeorological variability will benefit water managers, flood forecasters, and civil protection authorities.

4. Discussion and Conclusions

The presence or absence of ARs significantly drives global hydrological variability, which occurs on seasonal and interannual timescales and is controlled by the frequency with which specific regions and catchments are affected by ARs in a hydrological year. Consistent with the original (global) formulation of ARs developed by Zhu and Newell (1998), also captured in the formulation by Guan and Waliser (2015), we find that the impacts of ARs extend beyond the extratropical areas commonly examined (e.g., western North America and Europe) and are also not restricted to the extratropics. We also recognize that other modes of climate variability may contribute to the flow events calculated here, but we are emphasizing the connection to extreme, synoptic horizontal transports (often referred to as Atmospheric Rivers). For example, as the above definitions were developed to include the transient, filamentary moisture transport in the Asian monsoon, the high-peak flow events detected in this region could include contribution from the monsoon flow. Similarly, this broad AR definition may also be applicable to areas where individual Low-Level-Jet (LLJ) features are linked with deep convection and consequently strong precipitation and high peak flows—albeit those specifically with long narrow "river-like" features of moisture transport. For instance, in the central United States, the AR known as "Maya Express" corresponds to the region of enhanced moisture transport within the Great Plains LLJ which has been connected to heavy precipitation in the area (Dirmeyer & Kinter, 2009; Lavers & Villarini, 2013). This potential connection between LLJs and ARs may also be observed in areas where this link has been documented such as India, Southeast Asia, Australia and Oceania, Southern Brazil, Chile, Central Africa, or Iran where ARs have been documented to overlap LLJs (Gimeno et al., 2016).

While a few previous reports highlight the major global impacts of ARs in coastal regions close to the areas where ARs make landfall (e.g., Guan & Waliser, 2015), our findings highlight that significant advection of moisture inland makes an important contribution to runoff, soil moisture, and snowpack accumulation (Figures 1a–1c) in many areas of the globe, and thus, ARs importantly shape global terrestrial hydrology. In the areas where AR-driven precipitation makes a significant contribution to the annual water supply, the prolonged absence of ARs may result in intense hydrological droughts. For instance, Dettinger (Dettinger & Cayan, 2014) attributed multidecadal drought in the California Delta, including the recent extreme drought, to fluctuations in precipitation arising from the lack of large AR-driven storms. In this study, we have identified areas across the globe which may be exposed to similar drought patterns. Our findings are also consistent with the paths of moisture that are thought to be the primary source for heavy precipitation in mountain ranges the U.S. Intermountain West as noted by (Alexander et al., 2015). Regionally, our findings also support the importance explored by (Rutz et al., 2015) of the evolution of ARs in the U.S West Coast.

Nonetheless, in our perturbed simulation, we do not account for the atmospheric implications of removing AR-driven precipitation. For instance, we do not alter the radiation fields to account for clouds that transport ARs-driven precipitation. Also, we do not account for further interactions between soil moisture and temperature at the near surface (Seneviratne et al., 2010). At the same time, the representation of plant responses in JULES has been found to leave wetter soils thus decreasing the likelihood of detecting droughts (Prudhomme et al., 2014). As a result, our drought estimates are conservative and our study provides a broad, global consideration of the hydrological impacts of ARs, which allows comparisons between one region to the other. Also, in our drought estimations we do not account for water management options such as water transfers that might be hampered by water deficits due to AR-related variability. For example, in California the Sierra Nevada contributes about 70% of the annual water supply to Los Angeles with a population of nearly 5 million people (Negin et al., 2015). In consequence, we presume that our estimates of the population exposed to droughts are underestimated as ARs indirectly amplify the propagation of drought risk into societies. Thus, we also acknowledge the existence of other types of droughts not addressed in this study (e.g., soil moisture drought or socioeconomic drought; see Van Loon, 2015) that may develop into more complex categories of droughts.

Similarly, we have identified global areas where the contribution of ARs to high flows may result in floods. Also, we find that in areas such as California, the Mississippi Catchment in the United States, Parana in Southern Brazil, the Murray-Darling basin in Australia, Turkey, and in areas of the Amur River in China, ARs are not only major contributors to high flow events and also via variability that leads to their absence but also they play an important role in the occurrence of hydrological droughts. Nonetheless, in spite of this, hydrological significance the skill associated with forecasts of AR-driven precipitation remains limited (Wick et al., 2013) and improvements in monitoring and modeling of these ARs offer scope for improving natural hazard risk reduction. The extent to which the global occurrence and intensity of ARs will be affected by future climate change is expected to increase; regional assessments have projected intensification owing to higher atmospheric moisture content under warming scenarios (e.g., Dettinger, 2011; Lavers et al., 2013).

Taken together, our findings demonstrate that through extreme horizontal moisture transfers, ARs exert a widespread and strong control on spatially heterogeneous patterns of hydrological variability to a greater extent than previously understood which enhances our understanding of hydrological risks. Improvements in the ability of models to predict ARs will be important for water resource management and flood hazard assessment and warrant further attention in the light of future climate change.

Acknowledgments

This work was supported by the National Aeronautics and Space Administration. This research in part was carried out on behalf of the Jet Propulsion Laboratory, California Institute of Technology. W. H. L. acknowledge funding support from the CAS President's International Fellowship Initiative (2017PC0068) and the National Key Research and Development Program of China (2016YFA0602402). Our model outputs containing the daily land surface hydrological variables for both the control and disturbed simulations are available here: https://figshare.com/s/97f8d14ed5fe66e74eb6. Also, our outputs containing the gridded extreme river flow and river depths values (control and disturbed) can be downloaded here https://figshare.com/s/fad4d001515e42ae17e9 and here https://figshare.com/s/d796d04c113c87c81c58, respectively.

References

Alexander, M. A., Scott, J. D., Swales, D., Hughes, M., Mahoney, K., & Smith, C. A. (2015). Moisture pathways into the U.S. intermountain west associated with heavy winter recipitation events. *Journal of Hydrometeorology*, *16*(3), 1184–1206. https://doi.org/10.1175/JHM-D-14-0139.1

Best, M. J., Pryor, M., Clark, D. B., Rooney, G. G., Essery, R. L. H., Ménard, C. B., … Harding, R. J. (2011). The Joint UK Land Environment Simulator (JULES), model description. Part 1: Energy and water fluxes. *Geoscientific Model Development*, *4*(1), 641–688. https://doi.org/10.5194/gmdd-4-641-2011

Blöschl, G., Ardoin-Bardin, S., Bonell, M., Dorninger, M., Goodrich, D., Gutknecht, D., … Szolgay, J. (2007). At what scales do climate variability and land cover change impact on flooding and low flows? *Hydrological Processes*, *21*(9), 1241–1247. https://doi.org/10.1002/hyp.6669

Blyth, E., Best, M., Cox, P., Essery, R., Boucher, O., Harding, R., … Woodward, I. (2006). JULES: A new community land surface model. *Global Change Newsletter*, *66*, 9–13.

Center for International Earth Science Information Network—CIESIN—Columbia University (2016). Gridded Population of the World, Version 4 (GPWv4): Population density adjusted to match 2015 revision UN WPP country totals.

Clark, D. B., & Gedney, N. (2008). Representing the effects of subgrid variability of soil moisture on runoff generation in a land surface model. *Journal of Geophysical Research*, *113*, D10111. https://doi.org/10.1029/2007JD008940

Cosby, B. J., Hornberger, G. M., Clapp, R. B., & Ginn, T. R. (1984). A statistical exploration of the relationships of soil moisture characteristics to the physical properties of soils. *Water Resources Research*, *20*(6), 682–690. https://doi.org/10.1029/WR020i006p00682

Dacre, H. F., Clark, P. A., Martinez-Alvarado, O., Stringer, M. A., & Lavers, D. A. (2015). How do atmospheric rivers form? *Bulletin of the American Meteorological Society*, *96*(8), 1243–1255. https://doi.org/10.1175/BAMS-D-14-00031.1

Dankers, R., & Feyen, L. (2009). Climate change impact on flood hazard in Europe: An assessment based on high-resolution climate simulations. *Journal of Geophysical Research*, *113*, D19105. https://doi.org/10.1029/2007JD009719

De Loe, R. C., & Kreutzwiser, R. D. (2000). Climate variability, climate change and water resource management in the Great Lakes. *Climatic Change*, *45*(1), 163–179. https://doi.org/10.1023/A:1005649219332

Dettinger, M. (2011). Climate change, atmospheric rivers, and floods in California—A multimodel analysis of storm frequency and magnitude changes. *Journal of the American Water Resources Association*, *47*(3), 514–523. https://doi.org/10.1111/j.1752-1688.2011.00546.x

Dettinger, M., & Cayan, D. R. (2014). Drought and the California Delta—A matter of extremes. *San Francisco Estuary Watershed Science*, *12*(2), 1–6.

Dirmeyer, P. A., & Kinter, J. L. (2009). The "Maya Express": Floods in the U.S. Midwest. *EoS Transactions of the American Geophysical Union*, *90*(12), 101–102. https://doi.org/10.1029/2009EO120001

Fischer, G., Nachtergaele, F., Prieler, S., van Velthuizen, H. T., Verelst, L., & Wiberg, D. (2012). Global Agro-ecological Zones Assessment for Agriculture (GAEZ 2008).
Ghanbarian-Alavijeh, B., Liaghat, A., Huang, G.-H., & Van Genuchten, M. T. (2010). Estimation of the van Genuchten soil water retention properties from soil textural data. *Pedosphere*, *20*(4), 456–465. https://doi.org/10.1016/S1002-0160(10)60035-5
Gimeno, L., Dominguez, F., Nieto, R., Trigo, R., Drumond, A., Reason, C. J. C., … Marengo, J. (2016). Major mechanisms of atmospheric moisture transport and their role in extreme precipitation events. *Annual Review of Environment and Resources*, *41*(1), 117–141. https://doi.org/10.1146/annurev-environ-110615-085558
Gimeno, L., Nieto, R., Vazquez, M., & Lavers, D. A. (2014). Atmospheric rivers: A mini-review. *Frontiers in Earth Science*, *2*, 1–6. https://doi.org/10.3389/feart.2014.00002
Gleick, P. H. (1989). Climate change, hydrology, and water resources. *Reviews of Geophysics*, *27*(3), 329. https://doi.org/10.1029/RG027i003p00329
Global Runoff Data Centre (2007). Major river basins of the world.
Guan, B., Molotch, N. P., Waliser, D. E., Fetzer, E. J., & Neiman, P. J. (2013). The 2010/2011 snow season in California's Sierra Nevada: Role of atmospheric rivers and modes of large-scale variability. *Water Resources Research*, *49*, 6731–6743. https://doi.org/10.1002/wrcr.20537
Guan, B., & Waliser, D. E. (2015). Detection of atmospheric rivers: Evaluation and application of an algorithm for global studies. *Journal of Geophysical Research: Atmospheres*, *120*(24), 12,514–12,535. https://doi.org/10.1002/2015JD024257
Gumbel, E. J. (1941). The return period of flood flows. *Annals of Mathematical Statistics*, *12*(2), 163–190. https://doi.org/10.1214/aoms/1177731747
Hirabayashi, Y., Mahendran, R., Koirala, S., Konoshima, L., Yamazaki, D., Watanabe, S., … Kanae, S. (2013). Global flood risk under climate change. *Nature Climate Change*, *3*(9), 816–821. https://doi.org/10.1038/nclimate1911
Kenyon, J., & Hegerl, G. C. (2010). Influence of modes of climate variability on global precipitation extremes. *Journal of Climate*, *23*(23), 6248–6262. https://doi.org/10.1175/2010JCLI3617.1
Lavers, D. A., Allan, R. P., Villarini, G., Lloyd-Hughes, B., Brayshaw, D. J., & Wade, A. J. (2013). Future changes in atmospheric rivers and their implications for winter flooding in Britain. *Environmental Research Letters*, *8*(3), 34010. https://doi.org/10.1088/1748-9326/8/3/034010
Lavers, D. A., & Villarini, G. (2013). Atmospheric rivers and flooding over the Central United States. *Journal of Climate*, *26*(20), 7829–7836. https://doi.org/10.1175/JCLI-D-13-00212.1
Lavers, D. A., & Villarini, G. (2015). The contribution of atmospheric rivers to precipitation in Europe and the United States. *Journal of Hydrology*, *522*, 382–390. https://doi.org/10.1016/j.jhydrol.2014.12.010
Marthews, T. R., Dadson, S. J., Lehner, B., Abele, S., & Gedney, N. (2015). High-resolution global topographic index values for use in large-scale hydrological modelling. *Hydrology and Earth System Sciences*, *19*(1), 91–104. https://doi.org/10.5194/hess-19-91-2015
McCabe, G. J., & Palecki, M. A. (2006). Multidecadal climate variability of global lands and oceans. *International Journal of Climatology*, *26*(7), 849–865. https://doi.org/10.1002/joc.1289
Mestas-Nuñez, A. M., & Enfield, D. B. (1999). Rotated global modes of non-ENSO sea surface temperature variability. *Journal of Climate*, *12*(9), 2734–2746. https://doi.org/10.1175/1520-0442(1999)012%3C2734:RGMONE%3E2.0.CO;2
Negin, A., Dzombak, D. A., & Small, M. J. (2015). Sustainability review of water-supply options in the Los Angeles region. *Journal of Water Resources Planning and Management*, *141*(12), A4015005. https://doi.org/10.1061/(ASCE)WR.1943-5452.0000541
Neiman, P. J., Schick, L. J., Ralph, F. M., Hughes, M., & Wick, G. A. (2011). Flooding in western Washington: The connection to atmospheric rivers. *Journal of Hydrometeorology*, *12*(6), 1337–1358. https://doi.org/10.1175/2011JHM1358.1
Prudhomme, C., Giuntolia, I., Robinson, E. L., Clark, D. B., Arnell, N. W., Dankers, R., … Wisser, D. (2014). Hydrological droughts in the 21st century, hotspots and uncertainties from a global multimodel ensemble experiment. *Proceedings of the National Academy of Sciences of the United States of America*, *111*(9), 3262–3267. https://doi.org/10.1073/pnas.1222473110
Ralph, F. M., & Dettinger, M. D. (2011). Storms, floods, and the science of atmospheric rivers. *Eos Transactions American Geophysical Union*, *92*(32), 265–266. https://doi.org/10.1029/2011EO320001
Ralph, F. M., Neiman, P. J., Wick, G. A., Gutman, S. I., Dettinger, M. D., Cayan, D. R., & White, A. B. (2006). Flooding on California's Russian River: Role of atmospheric rivers. *Atmospheric Sciences*, *33*(13), 2–6. https://doi.org/10.1029/2006GL026689
Ramos, A. M., Tomé, R., Trigo, R. M., Liberato, M. L. R., & Pinto, J. G. (2016). Projected changes in atmospheric rivers affecting Europe in CMIP5 models. *Geophysical Research Letters*, *43*, 9315–9323. https://doi.org/10.1002/2016GL070634
Rutz, J. J., Steenburgh, W. J., & Ralph, F. M. (2015). The inland penetration of atmospheric rivers over western North America: A Lagrangian analysis. *Monthly Weather Review*, *143*(5), 1924–1944. https://doi.org/10.1175/MWR-D-14-00288.1
Seneviratne, S. I., Corti, T., Davin, E. L., Hirschi, M., Jaeger, E. B., Lehner, I., … Teuling, A. J. (2010). Investigating soil moisture–climate interactions in a changing climate: A review. *Earth-Science Reviews*, *99*(3–4), 125–161. https://doi.org/10.1016/j.earscirev.2010.02.004
Sheffield, J., & Wood, E. F. (2011). *Drought: Past problems and future scenarios*. London: Earthscan Ltd.
Trenberth, K. E. (2005). The impact of climate change and variability on heavy precipitation, floods, and droughts. *Encyclopedia of Hydrological Sciences*, *1–11*. https://doi.org/10.1002/0470848944.hsa211
Van Loon, A. F. (2015). Hydrological drought explained. *WIREs Water*, *2*(4), 359–392. https://doi.org/10.1002/wat2.1085
Viale, M., & Nuñez, M. N. (2011). Climatology of winter orographic precipitation over the subtropical central Andes and associated synoptic and regional characteristics. *Journal of Hydrometeorology*, *12*(4), 481–507. https://doi.org/10.1175/2010JHM1284.1
Viles, H. A., & Goudie, A. S. (2003). Interannual, decadal and multidecadal scale climatic variability and geomorphology. *Earth-Science Reviews*, *61*(1–2), 105–131. https://doi.org/10.1016/S0012-8252(02)00113-7
Weedon, G. P., Balsamo, G., Bellouin, N., Gomes, S., Best, M. J., & Viterbo, P. (2014). The WFDEI meteorological forcing data set: WATCH forcing data methodology applied to ERA-Interim reanalysis data. *Water Resources Research*, *50*, 7505–7514. https://doi.org/10.1002/2014WR015638
Wick, G. A., Neiman, P. J., Ralph, F. M., & Hamill, T. M. (2013). Evaluation of forecasts of the water vapor signature of atmospheric rivers in operational numerical weather prediction models. *Weather and Forecasting*, *28*(6), 1337–1352. https://doi.org/10.1175/WAF-D-13-00025.1
Yamazaki, D., Kanae, S., Kim, H., & Oki, T. (2011). A physically based description of floodplain inundation dynamics in a global river routing model. *Water Resources Research*, *47*, W04501. https://doi.org/10.1029/2010WR009726
Zhu, Y., & Newell, R. E. (1998). A proposed algorithm for moisture fluxes from atmospheric rivers. *Monthly Weather Review*, *126*(3), 725–735. https://doi.org/10.1175/1520-0493(1998)126%3C0725:APAFMF%3E2.0.CO;2